

2024

Role of phosphate restriction in regulating HIPPO and hypoxia signaling pathway gene expression during bone fracture repair

<https://hdl.handle.net/2144/51408>

"Downloaded from OpenBU. Boston University's institutional repository."

BOSTON UNIVERSITY

ARAM V. CHOBANIAN & EDWARD AVEDISIAN SCHOOL OF MEDICINE

Thesis

**ROLE OF PHOSPHATE RESTRICTION IN REGULATING HIPPO AND
HYPOXIA SIGNALING PATHWAY GENE EXPRESSION DURING BONE
FRACTURE REPAIR**

by

HANNA MOCHIDA

B.A., Boston University, 2022

Submitted in partial fulfillment of the
requirements for the degree of
Master of Science

2024

Approved by

First Reader

Louis C. Gerstenfeld, Ph.D.
Professor of Orthopaedic Surgery

Second Reader

Beth C. Bragdon, Ph.D.
Assistant Professor of Orthopedic Surgery

ACKNOWLEDGMENTS

I would like to thank Dr. Gerstenfeld for giving me the opportunity to conduct this research and Dr. Bragdon for serving as the second reader.

**ROLE OF PHOSPHATE RESTRICTION IN REGULATING HIPPO AND
HYPOXIA SIGNALING PATHWAY GENE EXPRESSION DURING BONE
FRACTURE REPAIR**

HANNA MOCHIDA

ABSTRACT

Bone, a hybrid tissue composed of carbonate-rich hydroxyapatite mineral and bone matrix proteins, serves various functions including mechanical support, metabolic homeostasis, and hematopoiesis. As hydroxyapatite is composed of calcium and phosphate, chronic phosphate deficiency or wasting leads to impaired skeletal mineralization. Phosphate is essential for mineralization, thus, an important regulator for the differentiation of chondrocytes. Previous studies showed hypophosphatemic conditions by food intake affect bone fracture healing process. Several recent studies implicated the involvement of a set of molecular metabolic/signaling pathways to control bone fracture healing process. However, the involvement of HIPPO and hypoxia signaling pathways during fracture healing with hypophosphatemic condition is still largely unknown. Therefore, the current study was conducted to test the hypothesis whether HIPPO and hypoxia signaling pathway is associated with the fracture healing process with dietary phosphate restriction.

In this study, we examine their involvement during fracture healing under control and hypophosphatemic conditions and analyze both gene and protein expression by quantitative real-time polymerase chain reaction (qPCR) and histological analyses. RNA

was isolated, purified, and used for reverse transcription to synthesize cDNA. The cDNA was then subjected to qPCR using specific primers for markers related to chondrogenesis, osteogenesis, phosphate regulation, HIPPO pathway, and hypoxia. Histological staining analyses were performed on femur samples to assess callus tissue formation and collagen matrix organization. Safranin-O staining, picro-sirius red staining, and immunohistochemical staining were conducted to evaluate cellular and matrix characteristics. The results provide insights into the effects of dietary phosphate restriction on the expression of key genes, the quality of callus extracellular matrix during bone fracture healing, oxidative metabolic collagen gene regulation, and HIPPO regulatory activity during bone fracture healing. The qPCR analysis revealed that phosphate restriction led to enhanced expression levels of chondrogenesis and early/intermediate osteogenesis markers, while late-stage osteogenesis marker expression was impaired. Additionally, phosphate restriction showed a differential effect on phosphate-regulation markers, inhibiting the expression of fibroblast growth factor 23 (FGF23) but leaving phosphate regulating endopeptidase homolog, X-linked (Phex), essentially unaffected. Furthermore, phosphate restriction markedly inhibited the expression levels of HIPPO signaling pathway markers.

Histological analysis demonstrated that phosphate restriction resulted in disorganized chondrocyte zones with more hypertrophic chondrocytes and inhibited collagen matrix organization and maturation during bone fracture healing. Immunohistochemical analysis revealed reduced immunoreactivity of type I collagen and connective tissue growth factor (CTGF) in the phosphate-restricted group compared to the control, indicating impaired

bone formation and reduced cellular activity. Other key findings included alterations in gene expression profiles, callus tissue formation, collagen matrix organization, and protein expression patterns of HIPPO and hypoxia markers during bone fracture healing. The findings suggested that phosphate restriction modulates the expression of YAP/TAZ target genes, potentially influencing fracture healing outcomes. The study also explored the effects of phosphate restriction on hypoxia signaling and collagen matrix quality during fracture healing. Overall, the results supported the hypothesis that dietary phosphate restriction inhibits the HIPPO and hypoxia signaling pathways, affecting the quality of callus extracellular matrix organization and maturation during bone healing. Future directions for research include investigating the regulation of collagen-modifying enzymes, examining additional YAP/TAZ target genes, and exploring hypoxia-related gene expressions to further elucidate the mechanisms underlying the effects of dietary phosphate restriction on fracture healing.

TABLE OF CONTENTS

ACKNOWLEDGMENTS	iv
ABSTRACT.....	v
TABLE OF CONTENTS.....	viii
LIST OF FIGURES	x
LIST OF ABBREVIATIONS.....	xi
INTRODUCTION	1
Bone.....	1
Bone matrix and mineral.....	1
Bone cells	2
Bone development and formation	3
Bone fracture healing.....	5
Role of phosphate in mineralization and fracture healing	11
MATERIALS AND METHODS.....	16
Quantitative Real-Time Polymerase Chain Reaction (qPCR).....	16
Synthesis of cDNA	16
Quantitative Real-Time PCR (qPCR).....	16
Histological staining analyses.....	18
Safranin-O staining	18
Picro-sirius red staining	19
Immunohistochemical staining analysis	19
RESULTS	21

qPCR analysis	21
Histological analysis: Safranin-O staining	28
Histological analysis: Picro-sirius red staining	30
Immunohistochemical analyses	32
Type I collagen staining.....	32
CTGF staining.....	33
DISCUSSION	36
REFERENCES	43
VITA.....	52

LIST OF FIGURES

Figure 1: Four phases of fracture healing associated with their gene expression	7
Figure 2: Stages of fracture repair	10
Figure 3: qPCR analysis: Chondrogenesis and osteogenesis markers	23
Figure 4: qPCR analysis: Phosphate-regulation markers	25
Figure 5: qPCR analysis: HIPPO signaling pathway markers	26
Figure 6: qPCR analysis: Hypoxia markers	28
Figure 7: Histological examination of mouse femur during fracture healing at day 10 and 21	29
Figure 8: Collagen matrix organization and maturation analyses of mouse femur during fracture healing at day 10 and 21	31
Figure 9: Immunohistochemical analysis with anti-collagen antibody during fracture healing at day 10 and 21	33
Figure 10: Immunohistochemical analysis with anti-CTGF antibody during fracture healing at day 10 and 21	35

LIST OF ABBREVIATIONS

Acan	Aggrecan
ANKRD1	Ankyrin Repeat Domain 1
ATP	Adenosine Triphosphate
AXL	Anexelekto
BGLAP	bone gamma-carboxyglutamate protein
BHLHB2	Basic helix-loop-helix family member e40
BMP	Bone Morphogenetic Protein
BNIP3	BCL2 Interacting Protein 3
BSP	Bone Sialoprotein
cDNA	complementary Deoxyribonucleic Acid
Colla1	Collagen type 1 alpha 1 chain
Colla2	Collagen type 1 alpha 2 chain
CTGF	Connective Tissue Growth Factor
CYR61	Cysteine-rich angiogenic inducer 61
dNTP	deoxyribonucleotide Triphosphate
ENO1	Enolase 1
FGF23	Fibroblast Growth Factor 23
Hif1 α	hypoxia-inducible factor 1- α
HRP	Horseradish Peroxidase
ICU	Intensive Care Unit
IL	Interleukin

MMP	Matrix Metalloproteinase
mRNA	messenger ribonucleic acid
MSC	Mesenchymal Stem Cell
mTLL	mammalian Tolloid Like
μg	micro-gram
μL	micro-litter
PBS	Phosphate Buffered Saline
PCR	Polymerase Chain Reaction
Phex	phosphate regulating endopeptidase homolog, X-linked
Pi	Phosphate
PMN	Polymorphonuclear Neutrophil
PTH	Parathyroid Hormone
P4ha1	prolyl 4-hydroxylase subunit alpha-1
P4ha2	prolyl 4-hydroxylase subunit alpha-2
qPCR	quantitative real time Polymerase Chain Reaction
REG	Regenerating Gene
RNA	Ribonucleic acid
RNase	Ribonuclease
rRNA	ribosomal Ribonucleic acid
RT	Reverse Transcription
Runx2	RUNX family transcription factor 2
SDF1	Stromal cell-Derived Factor 1

Taz..... Transcriptional coactivator with PDZ-binding motif
TGF-beta..... Transforming Growth Factor-beta
TNF-alpha..... Tumor Necrosis Factor-alpha
VEGF Vascular Endothelial Growth Factor
YAP Yes Associated Protein

INTRODUCTION

Bone

Bone is a hybrid bio-material, composed of carbonate-rich hydroxyapatite and bone matrix proteins, mainly type I collagen matrix. This “hybrid” tissue serves as a 3 dimensional template for its various functions. The function of bone consists of mechanical support, protection of the vital and internal organs, metabolic homeostasis by the reservation of ions such as calcium and phosphate, and hematopoiesis.

Developmentally there are two types of bone formation; intramembranous ossification for flat bones and endochondral ossification for long bones. Structurally, bone is further classified into cortical and trabecular bone. Bone is composed of cells and extracellular matrix like any other connective tissue and all types of bone consist of the same cells and matrix contents. The main difference lies in their structure and function with 80-90% of cortical bone volume composed of calcified matrix in contrast to trabecular bone which is only 15-25% mineralized matrix with the remaining volume composed of bone marrow, stromal connective tissues, and blood vessels (Bilezikian, 2019).

Bone matrix and mineral

70% of the bone extracellular matrix is composed of inorganic components, and 30% of organic contents. The inorganic matrix contains hydroxyapatite spindle-like crystals $\text{Ca}_{10}(\text{PO}_4)_6(\text{OH})_2$, which accounts for 95% of the total minerals and is frequently carbonated in humans. The organic matrix contains mostly collagenous proteins, predominantly type I collagen (85%) and non-collagenous proteins (15%). In bone

matrix, non-collagenous proteins have roles in cell binding, fibrillogenesis, promoting and regulating mineralization and crystal growth, and controlling bone resorption (Bilezikian, 2019).

Bone cells

Bone has three distinct types of cells; osteoblasts that form new bone, osteocytes the most abundant cell in bone tissues that regulate bone's functional activities, and osteoclasts which are the bone resorbing cell derived from a hematopoietic origin (Sommerfeldt & Rubin, 2001).

Osteoblasts are mononucleated, cuboidal cells that form bone by producing bone matrix components of collagen and ground substances, that subsequently goes through mineralization. Osteoblasts are found in clusters along the surface of the bone matrix they are secreting which is yet to be calcified. Osteoblasts originate from mesenchymal stem cells, such as the osteoprogenitor cells that reside in bone marrow and periosteum. The lineage of the stem cells differentiation into osteoblasts is controlled by expression of specific genes in a timely manner. Osteoblasts are histologically characterized by a basal round nucleus, a prominent Golgi, and abundant endoplasmic reticulum, which reflects the fact that these cells are very metabolically active. Osteoblasts not only have this role in bone formation, but also participate in regulating the osteoclastogenesis (Bilezikian, 2019).

Osteocytes are the most abundant cell in bone, consisting of 90-95% of total bone cells, and are considered the terminal differentiated osteoblasts. In comparison to

osteoblasts, they contain less organelles and are therefore smaller. Osteocytes are located in lacunae, where a calcified bone matrix surrounds them. As a result of their location inside the bone matrix and its cytoplasmic processes called canaliculi, osteocytes have a mechanosensory and regulatory function in controlling bone mass (Dallas, Prideaux, & Bonewald, 2013).

Osteoclasts specialize in bone resorption and are derived from mononuclear cells of the hematopoietic stem cell lineage. It is known that their cell differentiation is stimulated by osteoprogenitor cells, such as osteoblasts, and osteocytes, and terminally differentiated into giant multinucleated cells (Boyle, Simonet, & Lacey, 2003).

Osteoclasts are found at active bone-remodeling sites within Howship's lacunae.

Osteoclasts have morphological characteristics consisting of multiple nuclei, primary and secondary lysosomes, endoplasmic reticulum, prominent Golgi, and a ruffled border which is adjacent to the bone surface. For the purpose of degrading calcified bone, osteoclasts produce proteolytic enzymes and hydrogen ions to create an acidic environment for these enzymes to function (Holtrop & King, 1977; Vaananen, Zhao, Mulari, & Halleen, 2000).

Bone development and formation

Bone development occurs by two mechanisms (Bilezikian, 2019; Sommerfeldt & Rubin, 2001): intramembranous ossification and endochondral ossification. During intramembranous ossification, a group of mesenchymal cells differentiate directly into preosteoblasts, and then consequently to osteoblasts. These cells create a woven bone that is characterized by collagen bundles and randomly distributed calcification patches.

Mesenchymal cells differentiate at the periphery and blood vessels merge which forms hematopoietic bone marrow. This woven bone undergoes a remodeling process and is replaced by mature lamellar bone (Percival & Richtsmeier, 2013).

During endochondral ossification, bone formation is initiated when mesenchymal cells condense and cluster, which differentiate into chondrocytes, or cartilage cells. The cells at the periphery form the perichondrium, which is the primary ossification center. The chondrocytes in the cartilage proliferates and forms the matrix, which is composed of type II collagen and aggrecan. Then, the chondrocytes in the cartilage become hypertrophic and cease proliferation, and produce type X collagen. They also secrete vascular endothelial growth factors (VEGF) which initiate the invasion of the blood vessels with osteoclasts. Mineralization occurs by perichondrial cells differentiating to osteoblasts, forming bone collars (Kronenberg, 2003; Ortega, Behonick, & Werb, 2004).

Through continuous chondrocyte proliferation, the cartilage mold increases further in length, which is primarily controlled by hypertrophic chondrocyte production. When the chondrocytes at specific places within growth plates cease proliferation and differentiate to mature hypertrophic chondrocytes, secondary ossification centers are formed. As the hypertrophic chondrocytes begin to attract the invasion of blood vessels, osteoclasts with the differentiated osteoblasts degrade the calcified cartilage matrix that is replaced by the trabecular bone matrix. Hypertrophic chondrocytes then undergo apoptosis. With the growth of long bones, chondrocytes proliferate between the primary and secondary ossification centers, and the cartilage at this time is called the growth plate or epiphyseal plate (Kronenberg, 2003). This growth plate is composed of three distinct

zones of cells: round periarticular chondrocytes in the resting zone, flat-forming chondrocytes in the proliferation zone, and hypertrophic chondrocytes in the hypertrophic zone (Kobayashi et al., 2005).

Bone fracture healing

Bone loss, as a result of osteoporosis, is one of the major health threats to our aged society. Worldwide, approximately one in three women and one in five men over 50 years old are expected to suffer from osteoporosis-related fractures in their lifetime (Sozen, Ozisik, & Basaran, 2017). Shi et al. reported “2 million fractures related to osteoporosis occurred in 2005 and that 3.5 million osteoporotic fractures will occur in 2025. The associated costs of these osteoporotic fractures were estimated to be \$19 billion in medical costs in 2005, with an anticipated increase to \$25.3 billion in 2025 (Shi, Foley, Lenhart, & Badamgarav, 2009)”. Therefore, to understand bone fracture healing processes at the cellular and molecular levels, intensive research has been conducted in human clinical studies and animal fracture healing models.

Bone is one of the few unique tissues that undergo regeneration in which both the original cell types and tissue structure are truly regenerated using the embryological mechanism that formed the initial tissue. The bone fracture healing process requires orchestrated cellular activities where several cell types are involved including immunoinflammatory cells, chondroprogenitors, osteoprogenitors, chondrocytes, osteoblasts and osteoclasts. Despite the timing of repair/regeneration being different, the previous report using mouse callus tissues showed that similar transcriptomic activities to human stem

cells were observed during the experimental bone fracture healing process (Bais et al., 2009). As the repair process is accelerated in smaller animals, the rodent fracture/surgical model has been widely used to study the mechanism of experimental bone repair/healing processes (Bonnarens & Einhorn, 1984).

Primary or direct fracture healing and secondary or indirect fracture healing are the two major bone fracture healing types. Primary fracture healing is uncommon and occurs without displacement of bone fragments. The fracture site is bridged by the Haversian system with little or no inflammatory response. The healing process is slow, taking a few months to a few years to achieve complete healing (Marsell & Einhorn, 2011). Secondary fracture healing is more common and generally has the following four sequential stages; (a) initial injury, (b) endochondral formation, (c) primary bone formation and (d) secondary bone formation. Figure 1 shows the schematic summary, which illustrates these four stages during bone fracture healing and their associated gene expression levels.



Figure 1. Four phases of fracture healing associated with their gene expression.

Fracture healing processes include four stage-biological phases that are also associated with four main tissue events: inflammation, periosteal response, cartilage resorption, and coupled remodeling. The relative levels of each gene expression examined by the Gerstenfeld laboratory are expressed by three line widths. Figure taken from Gerstenfeld et al., 2003 (Gerstenfeld, Cullinane, Barnes, Graves, & Einhorn, 2003).

This fracture healing type involves immunological response to the injury followed by tissue anabolic and catabolic events. As the initial injury response to a bone fracture occurs in the bone marrow space, the blood supply is disrupted at the defect and hematoma forms near the disjunction (Einhorn, 1995). As a bone fracture causes acute inflammation, pro-inflammatory cytokines are produced including TNF-alpha, IL-1, and -6, which leads to further recruitment of immuno-inflammatory cells from hematopoietic origin such as macrophages, monocytes, polymorphonuclear neutrophils (PMNs) and lymphocytes. As the fracture healing process progresses, necrotic cells and tissue debris removal occurs mainly by PMNs and M1 macrophages. During the resolution of acute inflammation, macrophages are shifting their phenotype to M2 and anti-inflammatory cytokines such as IL-4, -10, and -13 are produced (Maruyama et al., 2020). Local cytokines such as TNF-alpha and stromal cell-derived factor 1 (SDF1) then work together with pro- and anti-inflammatory cytokines and several growth factors such as TGF-beta, BMPs and vascular endothelial growth factor (VEGF) to initiate a reparative fibrocartilaginous tissue formation (Maruyama et al., 2020).

Periosteum is considered as a well-vascularized connective tissue covering the cortical bone's outer surface. There are two layers, one is an outer, fiber-rich layer that contains cells (fibroblasts) and Sharpey fibers, allowing it to connect to the underlying cortical bone and an inner cambium layer. The cambium layer is enriched with mesenchymal stem cells (MSCs) and chondro- / osteo-progenitor cells (Orwoll, 2003). The periosteal progenitor cells then respond to the inflammation and undergo the chondrogenic differentiation or osteogenic differentiation (Einhorn & Gerstenfeld, 2015).

Chondroprogenitor cells are recruited to differentiate into chondrocytes which facilitate the endochondral bone formation. This occurs adjacent to the injured site by bone fracture where partial pressure of oxygen is low and the surrounding tissue is hypoxic, while osteoprogenitor cells are recruited and differentiate into osteoblasts, facilitating the intramembranous bone formation process. This takes place distal to the fracture site where intact blood supply remains. Indeed, chondrocytic fetal growth plate is virtually avascular and several hypoxia target factors positively regulate early chondrocyte differentiation (Provot et al., 2007). As the cell population expands and the fibrocartilaginous tissue forms, cross-sectional area and volume of this reparative growth are increased, referred to as the soft callus. As the inflammation phase resolves, the repair phase overlaps and endochondral bone formation takes place by recruiting bone marrow-derived MSCs. Similar to the embryological endochondral ossification process, chondrocytes are differentiated from the MSCs and proliferating chondrocytes produce cartilaginous matrix proteins such as type II collagen. As these chondrocytes further undergo cell differentiation and become hypertrophic chondrocytes, upregulation of type X collagen, CTGF and matrix metalloproteinase 13 (MMP13) is observed accompanied by angiogenic factor (VEGF)-mediated neovascularization tissue remodeling (Ortega et al., 2004). Cartilage matrix is subsequently mineralized and finally hypertrophic chondrocytes undergo programmed cell death, leading to the vascular invasion and osteoblast cell migration. Cartilage matrix subsequently converts to bone matrix, thus bony callus is formed. Concomitantly, osteoclast-driven coupled remodeling occurs and this catabolic event enables cross sectional area and volume of callus being decreased.

Now, at the late stage of bone fracture healing, newly formed bone is supposed to restore its original tissue structure, tissue shape, and mechanical property. Although the process is initiated as early as 3–4 weeks in animal and human models, the remodeling may take years to be completed to achieve a fully regenerated bone structure (Marsell & Einhorn, 2011). Figure 2 shows histological images at various stages of bone fracture healing.

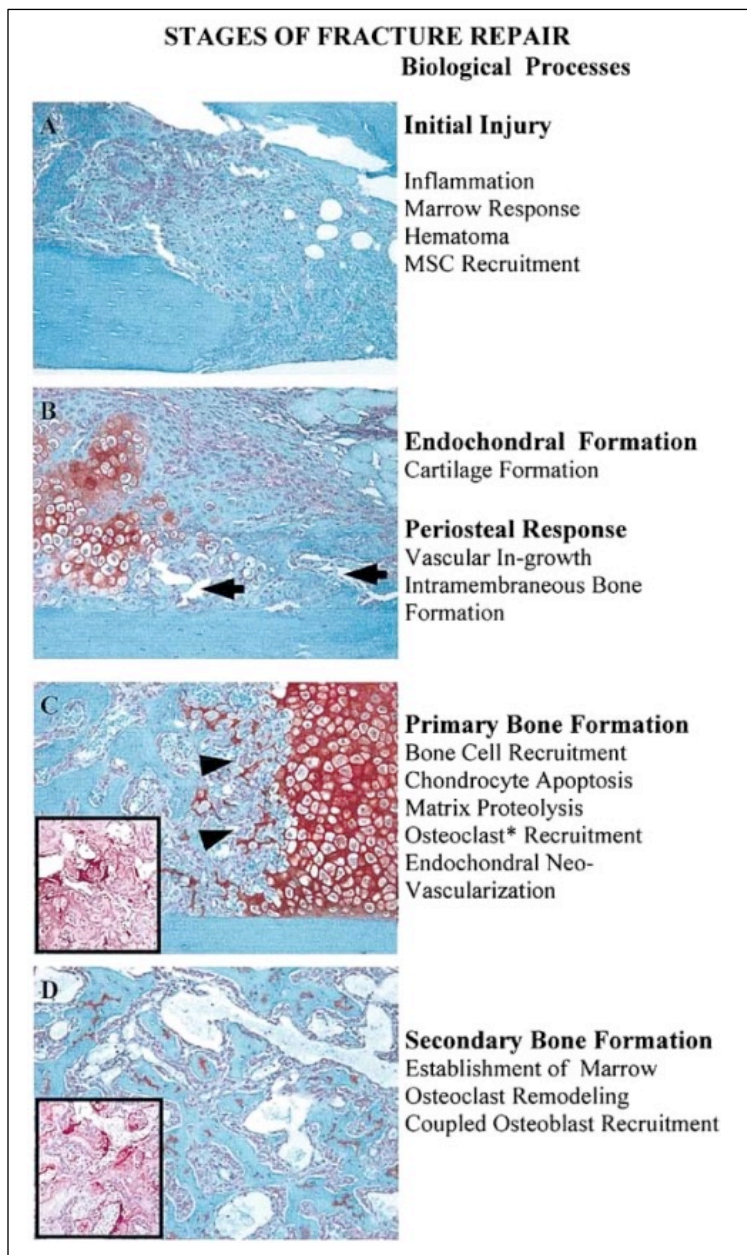


Figure 2. Stages of fracture repair. The following figure legend was taken from Gerstenfeld et al., 2003; “Specimens utilized for histologic analysis came from the sagittal plane of a mouse tibia that was fractured in the transverse plane. Magnification is 200X. Safranin O and fast green were the stains used. A. 24 hours post fracture. B. Preliminary response of the periosteum with endochondral formation 7 days after fracture. Arrows point to vascular ingrowth to fracture site. C. Primary bone formation 14 days following fracture. Arrows indicate new vascular ingrowth. Inset shows osteoclast resorbing calcified cartilage. D. 21 days after fracture. Inset depicts osteoclast resorbing primary bone.” Figure taken from Gerstenfeld et al., 2003 (Gerstenfeld et al., 2003).

Role of phosphate in mineralization and fracture healing

Phosphorus is naturally present in many foods. It is found either as phosphates or phosphate esters form in many types of foods. Usually in the United States, people take more phosphorus than they require through their dietary sources. However, some populations such as premature babies, people with certain genetic disorders, and with severe malnutrition, have insufficient amount of phosphorus. Although examination of phosphorus amount is atypically, phosphate can be measured in both serum and plasma, where about 55 % is in a free phosphate form, 35 % is combined with small cations, and 10 % is in a protein-bound form. In adults, phosphate concentration in serum or plasma ranging from 2.5 to 4.5 mg/dL (0.81 to 1.45 mmol/L) is considered as normal (Liamis, Milionis, & Elisaf, 2010). Since hydroxyapatite is composed of calcium and phosphate,

chronic phosphate deficiency or wasting results in impaired bone mineralization often seen in rickets, and osteomalacia (Michigami & Ozono, 2019).

A condition with serum phosphate concentration above the higher end of the standard values is considered hyperphosphatemia. It was reported that treatment of an elevated level of inorganic phosphate induces apoptosis in chicken hypertrophic chondrocytes in vitro (Mansfield, Rajpurohit, & Shapiro, 1999; Pucci et al., 2007). Furthermore, experimental phosphate addition to primary hypertrophic chondrocyte culture led to activation of caspase-9, a mediator of the mitochondrial apoptotic pathway (Sabbagh, Carpenter, & Demay, 2005). On the other hand, a condition with serum phosphate concentration below the lower end of the standard values is considered hypophosphatemia, which can be acute or chronic. Certain conditions such as alcoholism, sepsis, or patients in intensive care units (ICUs), may induce acute hypophosphatemia and the incidence varies 30 – 50 %. In chronic hypophosphatemic conditions, young patients manifest abnormal growth and rickets, while adult patients show osteomalacia, due to genetic or acquired phosphate-wasting diseases (Felsenfeld & Levine, 2012). Using a mouse model of a rare genetic disease, X-linked hypophosphatemia (Hyp mouse), or an experimentally induced hypophosphatemia by low-phosphate/high-calcium diet, the study showed the reduction of active caspase-3 positive hypertrophic chondrocytes in vivo (Sabbagh et al., 2005). This observation is consistent with the results by enhanced apoptosis with phosphate treatment in hypertrophic chondrocytes in vitro (Mansfield et al., 1999; Pucci et al., 2007). Histological analysis using Hyp mouse showed that a hypertrophic chondrocyte layer of the growth plate was significantly

increased (Sabbagh et al., 2005). Similarly, the low-phosphate/high-calcium diet-induced hypophosphatemia also resulted in a marked expansion of the hypertrophic layer (Sabbagh et al., 2005). These observations and findings indicate the crucial role of phosphate either induced by diet or genetically on chondrocyte cellular function.

It is well accepted that phosphate is essential for mineralization, thus, an important regulator for the differentiation of chondrocytes. Moreover, recent studies indicate how hypophosphatemic condition by food intake affects the fracture healing process. Prior studies from our laboratory demonstrated that hypophosphatemia by low-phosphate diet is associated with the impaired bone healing that was in part mediated by altering chondrocyte differentiation via their impaired BMP-2 signaling (Wigner et al., 2010). Several recent studies also implicated the involvement of a set of molecular circadian rhythm genes, as it was known that skeletal tissues exhibit a robust circadian clock expression and that the metabolic functions of bones are regulated in a circadian fashion (Aoyama & Shibata, 2017; Zvonic et al., 2007). Notably, growth plate tissues including chondrocyte layers exhibited a marked expression level of circadian clock genes and their oscillation was regulated by PTH directly (Kunimoto et al., 2016; Okubo et al., 2013). The transcriptomic analysis was performed using the mouse callus tissues with a normal amount of phosphate containing diet and phosphate restricted diet. The study revealed that the expression levels of major transcription factor genes involved in circadian rhythm molecular pathways were highly elevated in mice with phosphate restriction. Interestingly, their higher expression levels were reversed and comparable to those with a normal diet following a change back to normal phosphate diet, although the

course of PTH expression in serum was essentially unchanged (Noguchi et al., 2018). Further analysis using mouse fracture callus tissues showed that mitochondrial dysfunction and oxidative phosphorylation, and that circadian rhythm and phosphate restriction appeared to regulate canonical apoptosis pathways (Noguchi et al., 2018), indicating that dietary phosphate controls the cell fate of chondrogenic stem cells located at the resting zone and also apoptosis possibly by regulating circadian rhythm gene function. Furthermore, a more recent study reported the transcriptomic analysis of the callus tissues after fracture healing using mice with a normal diet and phosphate restricted diet (Hussein et al., 2023). The results demonstrated that genes associated with mitochondrial oxidative phosphorylation pathway and multiple intermediate metabolism pathways were regulated by systemic phosphate restriction regardless of genetic background (Hussein et al., 2023). The C3H10T1/2 murine pluripotent stem cells were cultured and maintained either with normal phosphate concentration or 25% of phosphate concentration, and the effect of BMP-2 treatment was assessed on DNA content, protein content, hydroxyproline content, chondrogenic gene expression, ATP production, and oxygen consumption. Under a reduced phosphate level in the cultured media, BMP-2 failed to increase only aggrecan gene expression, while all other metabolic activities were unchanged (Hussein et al., 2023), indicating other intracellular signaling pathway(s) may directly regulate mitochondrial function. In this study, we expand on our prior work and examine two of the signaling processes, HIPPO and HIF1 α (Koo & Guan, 2018; Y. Li, Yang, Qin, & Yang, 2021; Sivaraj et al., 2020) that we had identified in our transcriptomic analysis. The current study was conducted to test the hypothesis whether

HIPPO and hypoxia signaling pathway is associated with the fracture healing process with dietary phosphate restriction. We examine their involvement during fracture healing under control and hypophosphatemic conditions and analyze both gene and protein expression of both direct mediators of their activity and down stream targets that are regulated by their activities.

MATERIALS AND METHODS

Quantitative Real-Time Polymerase Chain Reaction (qPCR)

Synthesis of cDNA

RNA used in this study was previously isolated, purified and assessed for intactness as previously reported (Noguchi et al., 2018). One μg of the total RNA from each time point sample was used for reverse transcription (RT) using the TaqMan Reverse Transcription Reagents (Applied Biosystems) to synthesize the first-strand cDNA as follows: 1 μg of the isolated RNA was prepared and RNase free water was added up to 10.4 μl . The reverse transcription reagents were prepared by mixing 10X RT Buffer, 25mM MgCl_2 , 10mM dNTP (2.5mM each), RNase inhibitor, Taqman reverse transcriptase, and random hexamers. Nineteen point six μl of the RT-PCR reagents were mixed with the 10.4 μl of each RNA sample, making up a total volume of up to 30 μl . The RNA and reverse transcription reagents mixture samples were incubated as follows; 25 °C for 10 minutes, 37 °C for 1 hour, 95 °C for 5 minutes, and held at 4 °C. The newly synthesized cDNA samples were then diluted with RNase free water at a ratio of 1:50 and stored at -20 °C until use.

Quantitative Real-Time PCR (qPCR)

The synthesized cDNA was used as a template for qPCR. The qPCR was performed in duplicate with Taqman MGB expression assays (Applied Biosystems) using an ABI 7700 Sequence Detector (Applied Biosystems). Ten μl of the Universal Master Mix (Applied Biosystems Cat# 4304437) and 1 μl of the primer-probe set were used to

make the primer-probe/master mix for each well. For each of the 96-well qPCR plates, 9 μ l of the diluted cDNA and 11 μ l of the primer-probe/master mix were used to make a total volume of 20 μ l per well. The 96-well plate was covered with a clear film (Applied Biosystems Cat# 4306311). To get rid of bubbles, the 96-well plate was centrifuged at 1500 rpm for 2 minutes. The qPCR cycle condition was programmed as follows: 50 °C for 2 minutes, 95 °C for 10 minutes, 95 °C for 15 seconds, 60 °C for 60 seconds, and repeated the cycle for 40 times.

The specific primers-probes for mouse osteogenesis, chondrogenesis, phosphate-regulation, HIPPO pathway and hypoxia markers were used and the relative expression level of each marker was normalized to that of 18s rRNA in the same sample. The chondrogenic differentiation was examined by examining the expression level of aggrecan (Acan). The osteoblast differentiation was evaluated by assessing the expression levels of the following markers: bone gamma-carboxyglutamate protein (BGLAP), bone sialoprotein (BSP) and collagen type 1 alpha 2 chain (Col1a2). The phosphate-regulating gene expression was investigated using the following markers: fibroblast growth factor 23 (FGF23) and phosphate regulating endopeptidase homolog, X-linked (Phex). The HIPPO pathway gene expression was investigated using the following markers: transcriptional coactivator with PDZ-binding motif (Taz), connective tissue growth factor (CTGF) and matrix metalloproteinase 16 (mmp16). The hypoxia gene expression was investigated using the following markers: hypoxia-inducible factor 1-alpha (Hif1-alpha/Hif1a) and prolyl 4-hydroxylase subunit alpha-2 (P4ha2).

Histological staining analyses

Microscopy was carried out on Olympus BX51 (Olympus America, Inc., Center Valley PA) with the 4 X, 10 X and 20 X objectives. Digital images were captured and analyzed using the cellSens Dimension software (version 4.1.0.0, Olympus America).

Safranin-O staining

Mouse femur samples from the phosphate restricted group and control group at day 10 and 21 were collected and sections from each group at each time point was prepared. At least three slides containing 5 sections per slide for each group were used for the following staining analysis. Sections were de-paraffinized with xylene three times for 10 minutes each, and rehydrated with a series of ethanol gradually (100 % ethanol for 5 minutes, 100 % ethanol for 2 minutes, 95 % ethanol for 2 minutes, and 75 % ethanol for 2 minutes), slides were then placed in distilled water for 5 minutes and blotted on paper towel. Sections were stained with Gill No.2 hematoxylin for 1 minute and washed in distilled water at least four times until the water became clear and flowed by blotting on a paper towel. Slides were immersed in fast green for 8 minutes followed by rinsing with 1% acetic acid solution for 10 seconds. Slides were further immersed in 0.1 % safranin-O for 10 minutes followed by rehydration with 95 % and 100 % ethanol for 2 minutes each and by clearing with xylene twice for 2 minutes each. Stained sections were photographed for analysis.

Picro-sirius red staining

The sections from the phosphate restricted group and control group at day 10 and 21 were prepared. Three slides containing 5 sections for each group were used for the following staining analysis. Sections were de-paraffinized with xylene three times for 10 minutes each, and rehydrated with a series of ethanol gradually (100 % ethanol for 5 minutes, 100 % ethanol for 2 minutes, 95 % ethanol for 2 minutes, and 75 % ethanol for 2 minutes), slides were then placed in distilled water for 5 minutes and blotted on paper towel. Samples were immersed in Picro Sirius Red Solution (Abcam, Cat# ab150681) for 60 minutes. Sections were rinsed with 0.5% acetic acid twice, rinsed with 100 % alcohol for 5 minutes, dehydrated with absolute alcohol for 5 minutes twice and then mounted using Permount mounting medium. Samples were observed using a polarization filter.

Immunohistochemical staining analysis

The sections from the phosphate restricted group and control group at day 10 and 21 were prepared. Three slides containing 5 sections for each group were used for the following staining analysis. Sections were de-paraffinized with xylene three times for 10 minutes each, and rehydrated with a series of ethanol gradually (100 % ethanol for 5 minutes, 100 % ethanol for 2 minutes, 95 % ethanol for 2 minutes, and 75 % ethanol for 2 minutes). Slides were placed in PBS for 5 minutes and blotted on paper towel. Antigen retrieval was performed by using a pH 9.0 Tris-based antigen unmasking solution (Vector Laboratories, Cat# H-3301). The Tris buffer was heated for 30 seconds at a time in a microwave until the solution reached a temperature of 95 °C. After reaching 95 °C, the

slides were placed into the glass jar and left to cool to room temperature. The slides were washed three times in PBS for 10 minutes each wash. The slides were incubated in BLOXALL Blocking Solution (Vector laboratories, Cat# SP-6000) for 10 minutes to quench endogenous peroxidase activity. Sections were washed with PBS for 5 minutes, and then incubated with 2.5 % of normal horse serum for 20 minutes, followed by a 30 minute incubation with the primary antibody diluted in buffer containing 1.5 % blocking serum. Primary antibodies used in this study are; anti-collagen type I antibody (Proteintech, 14695-1-AP) and anti-CTGF antibody (PA5-32193, Invitrogen). sections were washed with PBS for 5 minutes, and then incubated for 30 minutes with the Biotinylated Universal Secondary Antibody. Sections were washed with PBS for 5 minutes, and incubated for 30 minutes with the R.T.U. VECTASTAIN Elite ABC-HRP Reagent (Vector laboratories, Cat# PK-7100). Sections were washed with PBS, and incubated in a peroxidase substrate solution until the desired immunoreactive intensity was developed. Sections were rinsed with PBS, counter-stained with hematoxylin, and mounted with PermOUNT mounting medium.

RESULTS

In order to examine how dietary phosphate restriction altered oxidative metabolic collagen gene regulation and HIPPO regulatory activity, two approaches were used. In the first set of studies, we examined mRNA expression for a series of genes associated with these three molecular functions. In the second part of our studies, we used histological and immunohistological approaches to examine aspects of collagen matrix synthesis and HIPPO regulatory activity.

qPCR analysis

To investigate the gene expression of various markers in the femur tissues, qPCR was performed (Figures 3-6).

The expression levels of a chondrogenesis marker including aggrecan (ACAN) and osteogenesis markers including collagen type 1 alpha 2 chain (Colla2), bone sialoprotein (BSP), and bone gamma-carboxyglutamate protein (BGLAP) were first investigated (Figure 3). In the normal diet (control) group, the expression of ACAN was increased, reached to a highest level at day 7, and was decreased to a baseline at day 18, while in the phosphate restricted (Pi) group, the expression was markedly increased, reached to a highest level (~ 3 fold higher than the control) at day 10, and was decreased to a baseline at day 21. The expression of Colla2 in the control group showed a higher baseline level at day 3, was decreased at day 10, and exhibited a biphasic peak at days 14 and 35, while in the Pi group, the expression was markedly increased from the zero baseline, reached to

a highest level at day 7 (~1.75 fold higher than the highest level in the control), and decreased at day 14. The expression of BSP in the control group was increased, reached to a highest level at day 10, and was decreased to a baseline at day 18, while in the Pi group, the expression exhibited a biphasic peak at days 7 and 14 with a higher peak at day 14, and decreased to a baseline at day 21. The expression of BGLAP in the control group exhibited a biphasic peak at days 14 and 21 with a higher peak at day 14, and decreased to a baseline at day 35, while in the Pi group, the expression started increasing at day 7, had a modest peak at day 10 (~1/3 fold of the highest level in the control), and decreased to a baseline at day 14.

The results indicate that phosphate restriction enhanced the levels of a chondrogenesis (ACAN) and early/intermediate osteogenesis (Colla2 and BSP) marker expression, while the expression level of the late stage osteogenesis marker (BGLAP) was markedly impaired.

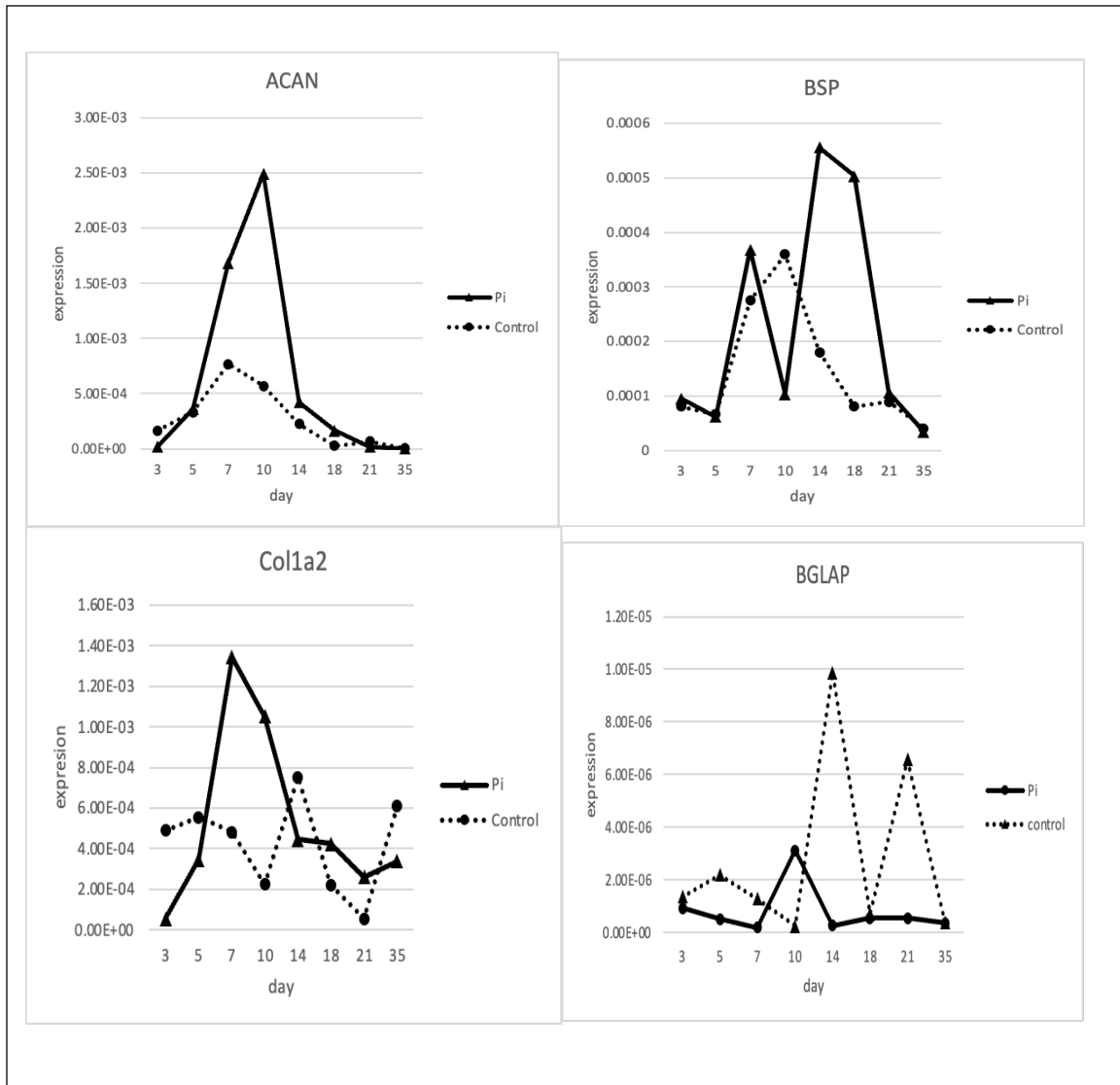


Figure 3. qPCR analysis: Chondrogenesis and osteogenesis markers. The graphs above show the temporal gene expression profiles of a gene associated with chondrogenesis (ACAN) and of three genes with osteogenesis (Col1a2, BSP, and BGLAP). Note that the black line indicates the profile with phosphate restricted diet while the dotted line with a normal diet.

The expression levels of phosphate-regulation markers including FGF23 and Phex were investigated (Figure 4). In the control group, the expression of FGF23 was markedly increased, reached to a highest level at day 5 (~2.5-3 folds higher than other two peaks in the control), was decreased to a baseline at day 10, and exhibited a biphasic peak at days 14 and 35, while in the Pi group, the expression remained at a minimum level throughout the time points tested. The expression of Phex in the control group exhibited a broader peak starting an increase at day 5, reached to highest levels at days 10-14, and was decreased to a baseline at higher baseline at day 21, while in the Pi group, the expression profile was almost similar to that of the control, showing a broader peak at days 14-18, and decreased to a baseline at day 35.

The results indicate that phosphate restriction showed a differential effect on the phosphate-regulation markers tested, i.e. the expression of FGF23 was markedly inhibited, while that of Phex was essentially unaffected.

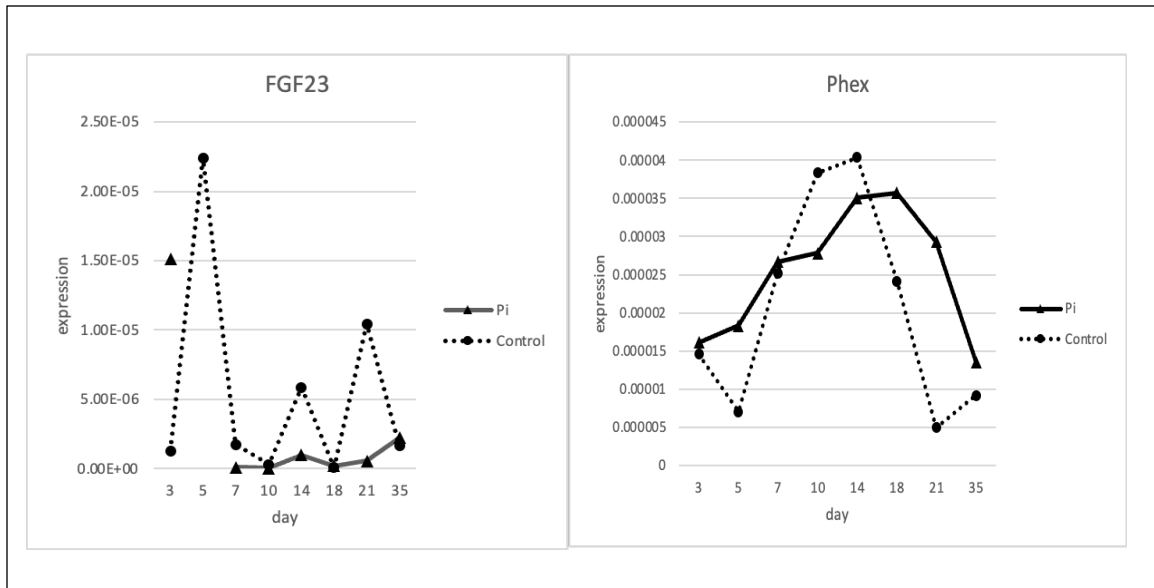


Figure 4. qPCR analysis: Phosphate-regulation markers. The graphs above show the temporal expression profiles of two phosphate-regulation genes (FGF23 and Phex). Note that the black line indicates the profile with phosphate restricted diet while the dotted line with a normal diet.

The expression levels of HIPPO signaling pathway markers including TAZ, mmp16, and CTGF were investigated (Figure 5). In the control group, the expression of TAZ was markedly increased, when it reached to its highest level at day 5 (~4.5 folds higher than the Pi), was decreased closer to a baseline at days 7-10, while in the Pi group, the expression remained at a minimum level throughout the time points tested. The expression of mmp16 in the control group exhibited a higher baseline level than the Pi group with a highest peak at day 14, while in the Pi group, the expression remained a higher baseline similar to that of the control with no distinct peak of the expression

throughout the time points tested. The expression of CTGF in the control group was markedly increased at its highest level at day 7 (~2.3 folds higher than the Pi), followed by a decrease closer to the baseline at day 10. In the Pi group, the initial expression level at day 3 was ~2 folds higher compared to the control, however, the expression decreased at day 5 and remained at a minimum level thereafter.

The results indicate that phosphate restriction markedly inhibited the expression levels of HIPPO signaling pathway markers used in this study.

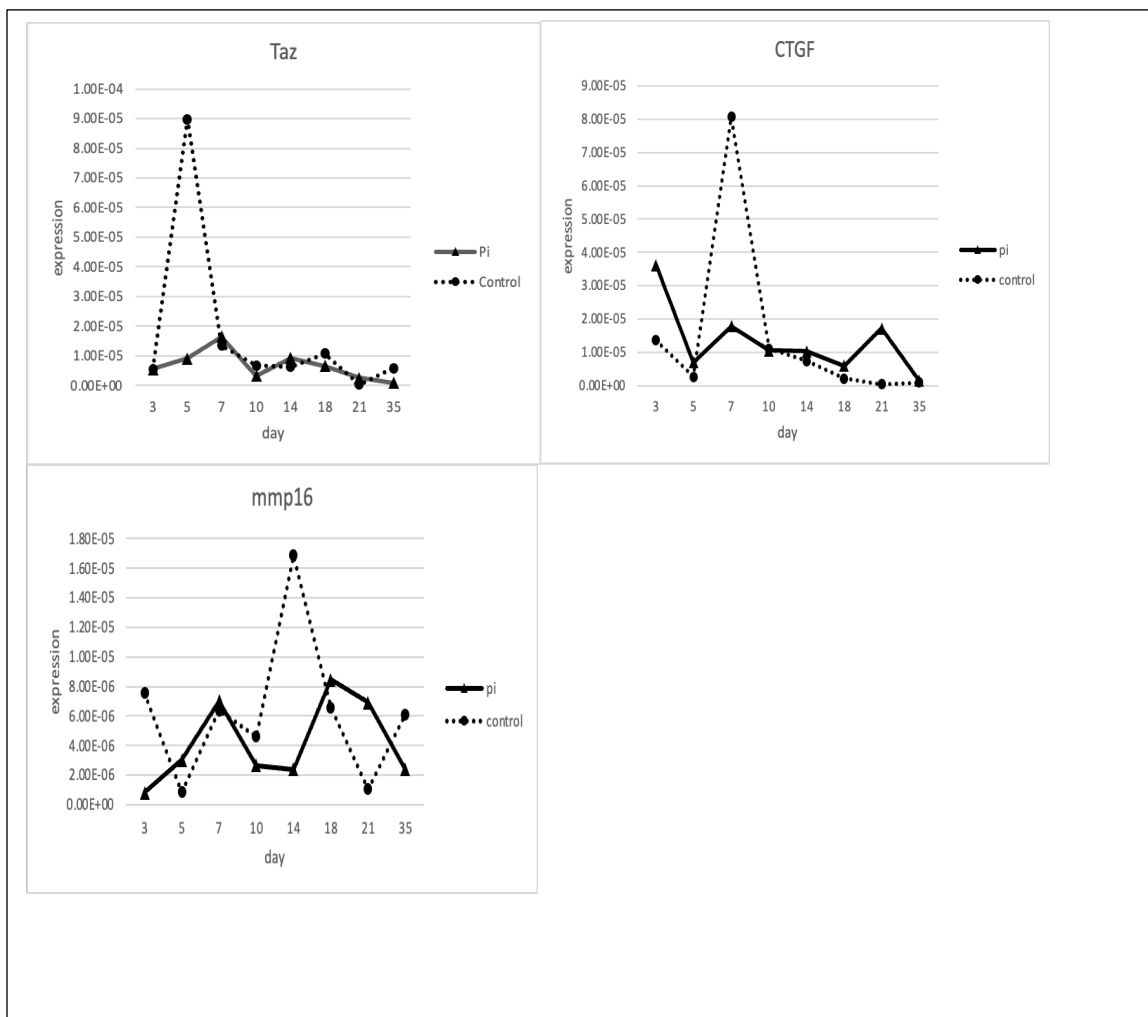


Figure 5. qPCR analysis: HIPPO signaling pathway markers. The graphs above show the temporal expression profiles of three HIPPO signaling pathway-associated genes (Taz, mmp16 and CTGF). Note that the black line indicates the profile with phosphate restricted diet while the dotted line with a normal diet.

The expression levels of hypoxia markers including hypoxia-inducible factor 1-alpha ($Hif1\alpha$) and prolyl 4-hydroxylase subunit alpha-2 (p4ha2) were investigated (Figure 6). In the control group, the expression of $Hif1\alpha$ showed multiple peaks at day 3, 7, 14 and 35, while the Pi group showed one large peak at day 7. The expression of p4ha2 in the control group exhibited increased expression at day 3, followed by decreased expression at day 7, that then increased again at day 10, and decreased closer to a zero baseline thereafter. The Pi group showed expression at day 3 that was higher than that of the control (~2 folds higher than the control), the expression was then markedly decreased closer to a zero baseline, and increased to exhibit a broader peak at days 7-18, and was decreased closer to a zero baseline at days 21 and 35.

The results indicate that phosphate restriction showed a differential effect on the hypoxia markers tested, i.e. the expression of $Hif1\alpha$ was modestly inhibited, while that of p4ha2 appeared to be slightly enhanced.

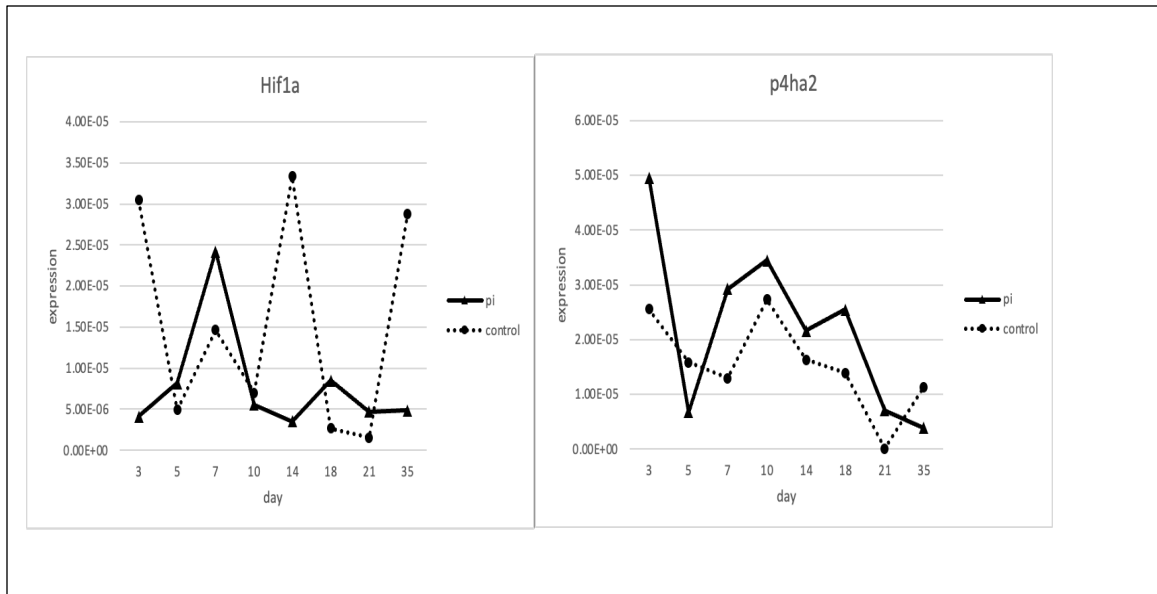


Figure 6. qPCR analysis: Hypoxia markers. The graphs above show the temporal expression profiles of two hypoxia-associated genes ($Hif1\alpha$ and $p4ha2$). Note that the black line indicates the profile with phosphate restricted diet while the dotted line with a normal diet.

Histological analysis: Safranin-O staining

Histological examinations of mouse femur with a normal diet (control; left panels) and a phosphate restricted diet (Pi; right panels) at day 10 (upper panels) and day 21 (lower panels) after bone fracture were shown in Figure 7. Sections were stained with safranin-O where cartilage/chondrocytes are stained in bright red, while bone is stained in pale blue.

The image from the control group at day 10 after bone fracture demonstrated that the callus tissues were occupied with more cartilage matrices (Figure 7, upper left panel)

as compared to the Pi group that showed disorganized chondrocyte zones occupied with more hypertrophic chondrocytes (Figure 7, upper right panel).

At day 21 after bone fracture, only a few areas with safranin-O positive chondrocyte zones were observed in the control group, and the majority of the callus tissue was stained in pale blue/blue, indicating active primary bone formation takes place (Figure 7, lower left panel). In the Pi group, most of the safranin-O positive areas disappeared and were replaced with the areas with primary bone tissues stained in pale blue (Figure 7, lower right panel).

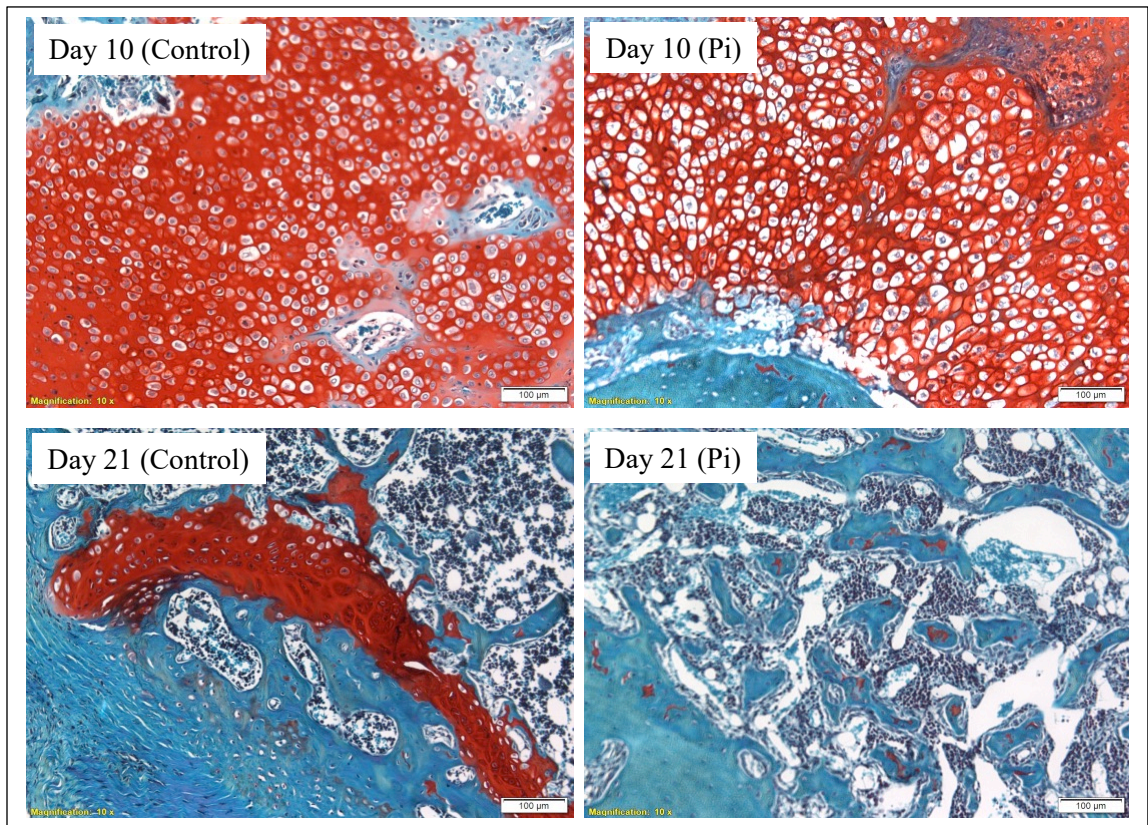


Figure 7. Histological examination of mouse femur during fracture healing at day 10 and 21. Mice with a normal diet (control) or phosphate restricted diet (Pi) were subjected to bone fracture and their femur samples were collected at day 10 and day 21 after the fracture. Sections were prepared to visualize the transverse plane of the femur and stained with safranin-O and fast green. Scale bar = 100 μm (magnification = 10 X).

Histological analysis: Picro-sirius red staining

The effect of phosphate restricted diet on collagen organization/maturation during bone fracture healing was examined by picro-sirius red staining at the light microscopic level. The images of mouse femur with a normal diet (control; Figure 8, left panels) and a phosphate restricted diet (Pi; Figure 8, right panels) at day 10 (Figure 8, upper panels) and day 21 (Figure 8, lower panels) after bone fracture are shown. Sections were stained with picro-sirius red to investigate the organization and directionality of collagen matrices and the extent of collagen matrix maturation where mature matrices are visualized in bright orange/red, while immature matrices in green/yellow.

At day 10, the organization of collagen matrix in the control group was uniform and colored mainly in red/bright orange (Figure 8, upper left panel), while in the Pi group, the collagen matrix was less organized and colored in pale red, yellow and green (Figure 8, upper right panel).

At day 21, the organization of collagen matrix in the control group became more organized, showing more uniform collagen fibers with directionality with dark red/bright orange color (Figure 8, lower left panel). In the Pi group, the collagen matrix showed

discontinuous directionality with thinner collagen fibers colored in red/bright orange (Figure 8, lower right panel). These results indicate that phosphate restriction inhibits the organization and maturation of collagen matrix during bone fracture healing process.

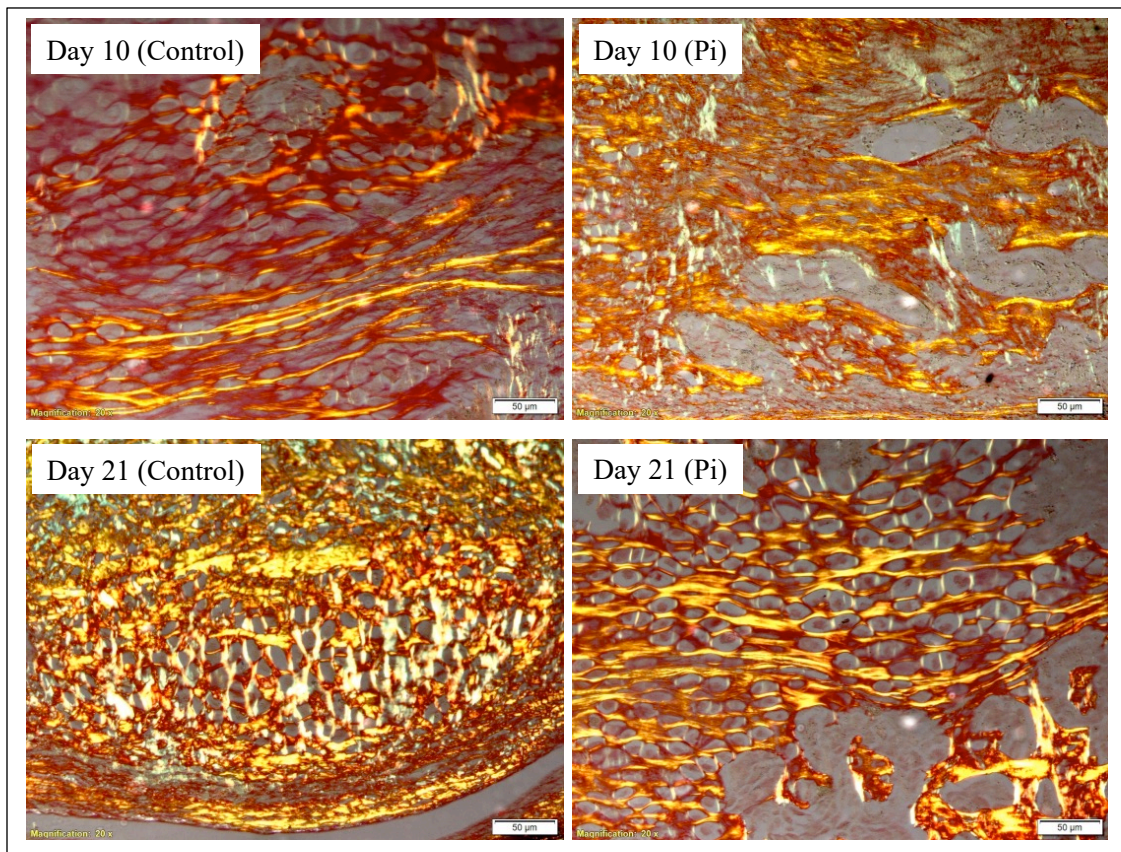


Figure 8. Collagen matrix organization and maturation analyses of mouse femur during fracture healing at day 10 and 21. Mice with a normal diet (control) or phosphate restricted diet (Pi) were subjected to bone fracture and their femur samples were collected at day 10 and day 21 after the fracture. Sections were prepared to visualize

the transverse plane of the femur and stained with picro-sirius red. The images were taken under a polarized microscope. Scale bar = 50 μm (magnification = 20 X).

Immunohistochemical analyses

Type I collagen staining

The qPCR analysis showed the temporal upregulation of Col1a2 gene during fracture healing in the phosphate restricted group (Figure 3). The immunohistochemical analysis using anti-collagen type I antibody was therefore performed using the mouse femur sections with a normal diet and phosphate restricted diet at day 10 and day 21 after bone fracture.

At day 10, in the control group, an intense immunoreactivity was observed in the area adjacent to the cluster of hypertrophic chondrocytes, indicating active bone formation takes place (Figure 9, upper left panel). On the other hand, in the Pi group, the extent of immunoreactivity in the area adjacent to the cluster of hypertrophic chondrocytes was much lesser than the control (Figure 9, upper right panel).

At day 21, in the control group, an immunoreactivity was observed on the surface and within the newly formed bone matrices (Figure 9, lower left panel), while in the Pi group, immunoreactivity observed was limited to the surface of bone matrices (Figure 9, lower right panel).

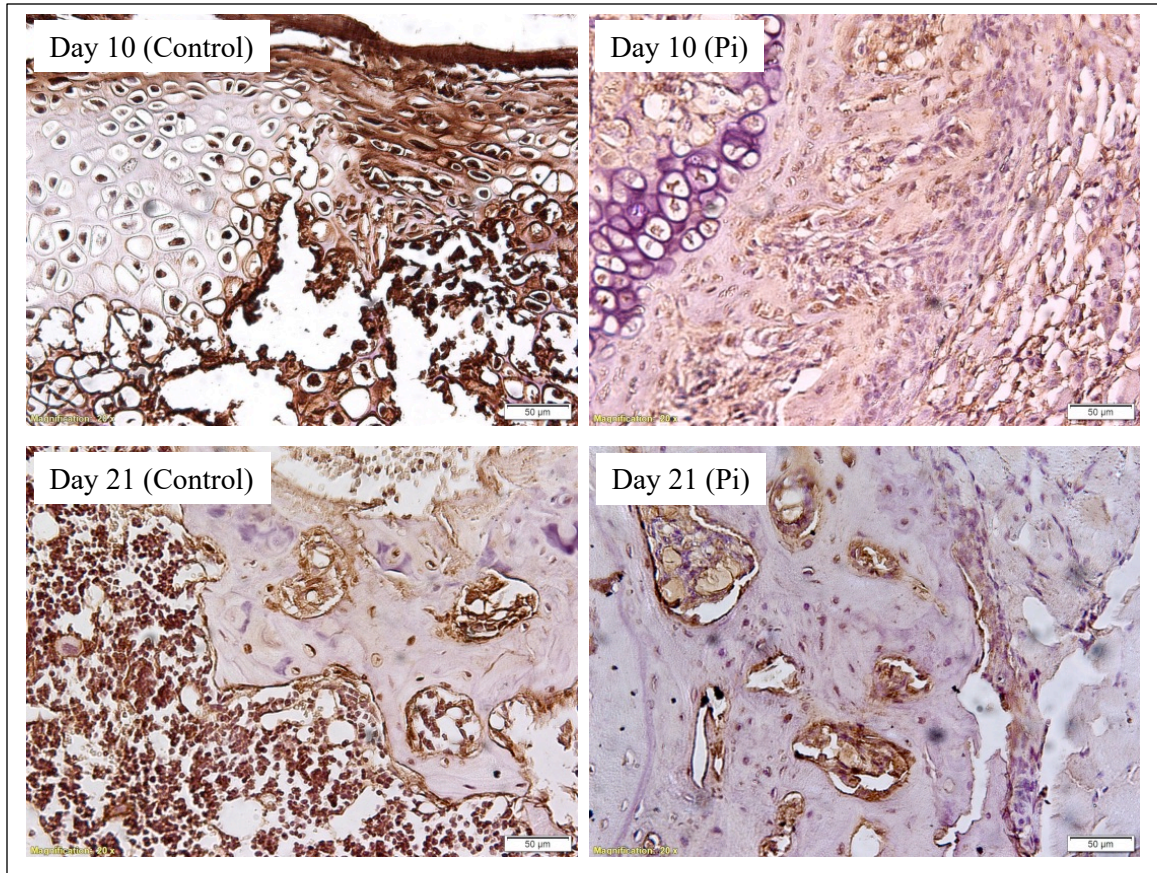


Figure 9. Immunohistochemical analysis with anti-collagen antibody during fracture healing at day 10 and 21. Mice with a normal diet (control) or phosphate restricted diet (Pi) were subjected to bone fracture and their femur samples were collected at day 10 and day 21 after the fracture. Sections were prepared to visualize the transverse plane of the femur and immunostained with anti-collagen type I antibody. Scale bar = 50 μ m (magnification = 20 X).

CTGF staining

The qPCR analysis showed the temporal upregulation of CTGF during fracture healing in the control group (Figure 5). The immunohistochemical analysis using anti-CTGF antibody was therefore performed using the mouse femur sections with a normal diet and phosphate restricted diet at day 10 and day 21 after bone fracture.

At day 10, in both of the control and Pi groups, no immunoreactivity was observed in the area adjacent to the cluster of hypertrophic chondrocytes (Figure 10, upper panels).

At day 21, in the control group, an immunoreactivity was observed within the several types of cells including osteoblasts, osteocytes and endothelial cells (Figure 10, lower left panel), while in the Pi group, weaker immunoreactivity was limitedly found within a very few osteoblasts and endothelial cells (Figure 10, lower right panel).

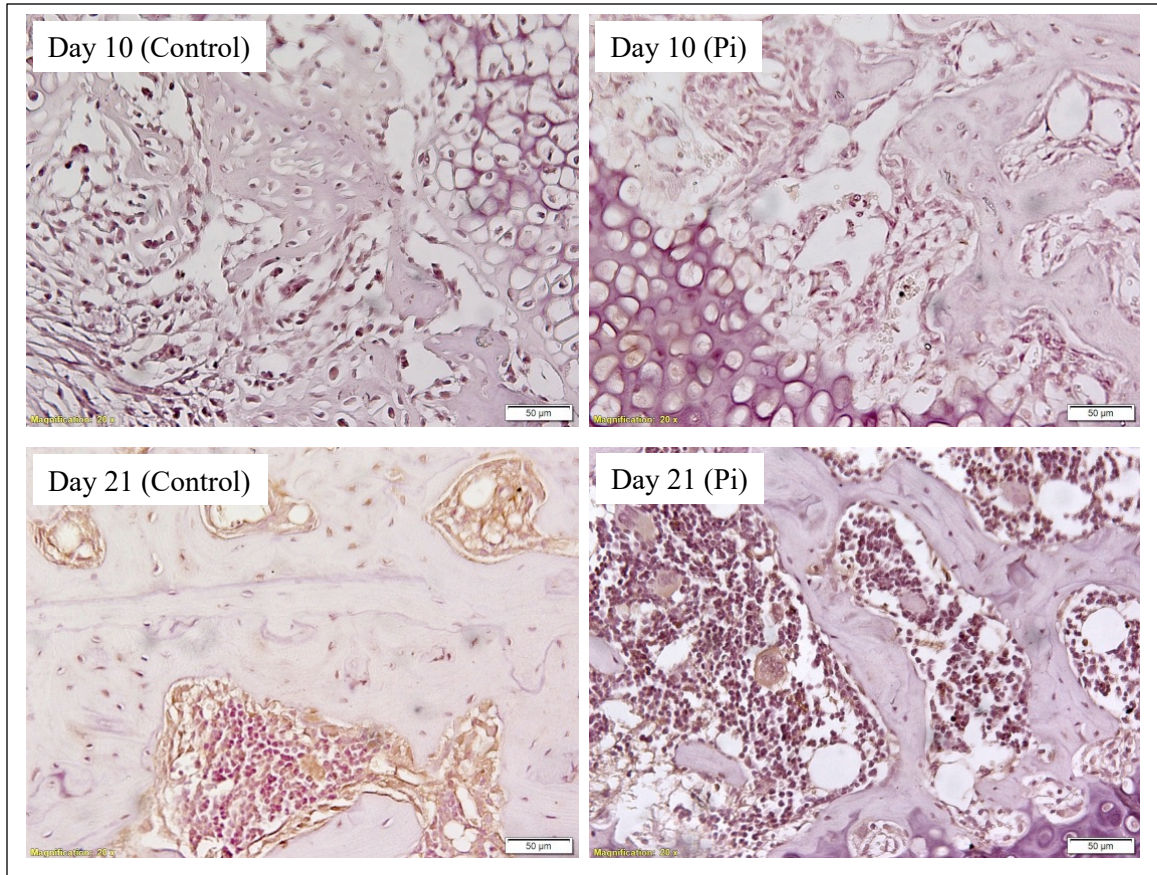


Figure 10. Immunohistochemical analysis with anti-CTGF antibody during fracture healing at day 10 and 21. Mice with a normal diet (control) or phosphate restricted diet (Pi) were subjected to bone fracture and their femur samples were collected at day 10 and day 21 after the fracture. Sections were prepared to visualize the transverse plane of the femur and immunostained with anti-CTGF antibody. Scale bar = 50 µm (magnification = 20 X).

DISCUSSION

Study findings

The current study was conducted to investigate whether the HIPPO and hypoxia signaling pathways are associated with the fracture healing process with dietary phosphate restriction. To test this hypothesis, the effect of dietary phosphate restriction was examined on the expression of a targeted set of genes during the callus tissue formation, which focused on collagen matrix organization and maturation, and protein expression pattern of HIPPO and hypoxia markers during bone fracture healing. As it is well accepted that coordinated cellular activities of several different cell types including immuno-inflammatory cells, chondroprogenitors, osteoprogenitors, chondrocytes, osteoblasts, and osteoclasts are all involved in the fracture healing process, the pattern of gene expression in the healing callus tissues is state-dependent, and thus the gene expression profile reflects the differentiation of these cell types.

Given that the endochondral healing process mirrors the developmental events within the skeleton, it is not surprising that the genetic profile partly resembles that observed in the hypertrophic program of growth plate chondrocytes. Aggrecan (ACAN) is a major cartilage extracellular matrix protein (Baldwin, Reginato, & Prockop, 1989) associated with hypertrophic chondrocyte differentiation. The temporal upregulation of ACAN gene expression was found in both control and Pi groups, although the time point of the highest expression was slightly different (control at day 7, while Pi at day 10) and its expression level was similarly decreased to almost a base-line at day 21 (Figure 3).

This expression pattern is consistent with the current histological finding that both control and Pi groups showed a notable increase in cell volume accompanied by hypertrophic chondrocytes and safranin-O positive matrices at day 10 (Figure 7, upper panels). Furthermore, at day 21, both control and Pi groups showed a decrease in safranin-O positive areas (Figure 7, lower panels). It is unclear as to why the peak expression of ACAN in the Pi group was higher than the control (Figure 3), as the previous reports showed a lower peak expression in the Pi than that of the control (Noguchi et al., 2018; Wigner et al., 2010).

There is also an overlay of genetic characteristics related to osteoblast differentiation, which is pertinent to both developmental long bone formation and endochondral healing process leading to the conversion of cartilaginous callus into woven bone. Notably, osteogenic markers including type I collagen, BSP, and BGLAP are detected. Both BSP and BGLAP are considered non-collagenous proteins synthesized by skeletal-associated cell types including chondrocytes and osteoblasts (Ducy & Karsenty, 1995; Fisher, McBride, Termine, & Young, 1990). The current data demonstrated that BGLAP expression in the control was markedly increased at day 14 and day 21, while in the Pi group, the extent of peak expression was generally suppressed (Figure 3). This is consistent with the previous report that BGLAP gene expression was upregulated at day 14 in the control group, while that was generally inhibited in the Pi group (Wigner et al., 2010). On the other hand, the expression of BSP in the Pi group showed a bi-phasic pattern and the peak expression was higher than the control (Figure 3), indicating that phosphate restriction affects the late osteoblast differentiation.

The extracellular matrix of connective tissue is a complex composite material with insoluble fibers, microfibrils, and a variety of soluble proteins and glycoproteins. The most major proteins of the extracellular matrix are the members of the collagen superfamily, and among them, type I collagen is the most abundant type of collagen, representing the principal fibrillar component of many tissues including bone. Type I collagen is a hetero-trimer consisting of two identical $\alpha 1$ chains (a product of the *Coll1a1* gene) and one $\alpha 2$ chain (a product of the *Coll1a2* gene). Previously, after 14 days of bone fracture, the type I collagen-expressing cells were decreased in the Pi group as compared to the control, suggesting that the phosphate restriction impairs osteoblast differentiation (Wigner et al., 2010). As in Figure 3, the current data of *Coll1a2* gene expression showed that at day 14, the expression of *Coll1a2* in the Pi was lower than that of the control, consistent with the previous report. However, the peak expression was much higher in the Pi than that of the control observed at day 7. Taken together with these osteogenesis marker results, the impairment of osteoblast differentiation by phosphate restriction may be a stage-dependent phenotype. Interestingly, the higher gene expression data of *Coll1a2* expression did not appear to correlate with the picro-sirius red staining data (Figure 8) and collagen immunohistochemical staining data (Figure 9). It is difficult to describe the quantity of collagen stained with picro-sirius red, thus it is difficult to compare the amount of collagen between control and Pi groups at day 10 (Figure 8, upper panels). However, as the picro-sirius staining data demonstrated a more disorganized collagen fibril pattern and poorer collagen maturation in the Pi group as compared to the control at both days 10 and 21, this strongly suggests that phosphate restriction led to the

impairment of collagen fibril structure, serving as a poor platform for bone fracture healing and re-mineralization. The anti-collagen type I antibody used in this study is raised against the C-terminal propeptide of the pro- α 2 chain. This suggests that the intense immunoreactivity in the control at day 10 is due to the detection of cleaved C-terminal pro- α 2 chain fragments embedded within the extracellular matrix. The higher gene expression of *Colla2* (Figure 3) with poorer immunoreactivity of collagen staining (Figure 9) in the Pi group at day 10 raises a possibility that the cleavage of C-terminal propeptide region may be inhibited, i.e. phosphate restriction could decrease the expression of collagen processing enzymes, such as BMP1, mTLL1, and mTLL2 proteinases (Kessler, Takahara, Biniaminov, Brusel, & Greenspan, 1996; S. W. Li et al., 1996; Scott et al., 1999).

Mammalian homologs of TAZ and YAP (Yes Associated Protein) are transcriptional cofactors (Kanai et al., 2000; Sudol et al., 1995). The YAP/TAZ complex is downstream of the HIPPO signaling pathway mediating crucial cellular functions such as cell differentiation, proliferation and apoptosis. Murine homolog of TAZ was molecularly cloned and it was shown that highest expression was observed in calvaria and skin by RT-PCR (Cui, Cooper, Yang, Karsenty, & Aukhil, 2003). According to the same report, TAZ interacted with Runx2, a master regulator of osteoblast differentiation (Ducy, Zhang, Geoffroy, Ridall, & Karsenty, 1997; Komori et al., 1997), and co-expression of TAZ with Runx2 enhanced Runx2-mediated activation of BGLAP reporter gene, indicating the importance of TAZ function in osteogenesis. YAP and TAZ were reported to regulate the mitochondrial size by controlling its fusion and fission (Nagaraj

et al., 2012; von Eyss et al., 2015), indicating the role of HIPPO pathway in mitochondrial metabolism. This notion is well coincided with the recent report that during bone fracture healing, phosphate restriction altered the mitochondrial oxidative phosphorylation (Hussein et al., 2023). The current study, therefore, investigated the effect of phosphate restriction on several YAP/TAZ target genes (Figure 5), by examining the expression levels of CTGF and MMP16 (Vanyai et al., 2020). The temporal upregulation of TAZ at day 5 in the control was observed, strongly correlating with the upregulation of CTGF at day 7 and MMP16 at day 14 (Figure 5), respectively. However, the expression of TAZ was generally suppressed by phosphate restriction, consistent with the data that CTGF and MMP16 upregulation were not observed. These data suggest that the temporal upregulation of TAZ could be crucial for its target gene expression and impairment of TAZ upregulation by phosphate restriction may account for abnormal fracture healing. CTGF was first identified in endothelial cells and fibroblasts (Bradham, Igarashi, Potter, & Grotendorst, 1991; Uhlen et al., 2015), and then was detected in many tissues including bone (Safadi et al., 2003). The immunohistochemical data using anti-CTGF antibody showed the temporal protein expression at day 21 in the control, but not Pi group, further confirming the notion that CTGF, a TAZ-target gene, expression was suppressed by phosphate restriction (Figure 10).

During bone fracture healing, the areas adjacent to the injured site by bone fracture have the lower partial pressure of oxygen due to disrupted vascular circulation, which is consistent with the concept that hypoxia is a crucial chondrogenesis inducer

(Provot et al., 2007). In addition, prolyl 4-hydroxylase, a collagen post-translational enzyme, is a target gene of Hif1 α (Bentovim, Amarilio, & Zelzer, 2012). The data showed that the expression of Hif1 α was modestly inhibited, while that of p4ha2 appeared to be slightly enhanced. This suggests that the gene expression of p4ha2 could be regulated not only by Hif1 α but also by another molecular mechanism. P4ha2 is one of the α subunit isoforms of the 2-oxoglutarate-dependent dioxygenases with a α 2- β 2 tetramer composition (Koski et al., 2017). Furthermore, as p4ha2 knockout mice show only a minor phenotype, p4ha1 is most likely capable of compensating for a loss of p4ha2 activity (Aro et al., 2015).

Conclusion and future directions

In conclusion, the current study supports the hypothesis that dietary phosphate restriction inhibits HIPPO and hypoxia signaling pathways during the bone fracture healing process. Furthermore, our data also suggested that dietary phosphate restriction likely modifies the quality of callus extracellular matrix organization and maturation during the bone healing process.

Our study can be further extended to the following studies. (1) As our data showed that phosphate restriction could decrease the quality of callus extracellular matrix organization and maturation, it is reasonable to speculate that this phenotypic change could be the result of altering the regulation of collagen modifying enzymes. Therefore, we could examine the expression of collagen processing enzymes, such as BMP1, mTLL1, and mTLL2 proteinases. To further extend such a study, it would be intriguing

to investigate the expression of collagen modifying genes and gene products, such as the collagen proteinases, prolyl-hydroxylases, lysyl hydroxylases and lysyl oxidases, during the course of bone fracture healing. The outcomes of such studies may bring a novel mechanistic insight into the role of dietary phosphate restriction in regulating the callus collagen matrix quality. (2) Our data showed the dramatic decrease of HIPPO signaling pathway gene expressions in the Pi group as compared to the control group. To further confirm our results, we could examine more YAP/TAZ target genes including CYR61, ANKRD1, REG, AXL, and MYC (Zarka, Hay, & Cohen-Solal, 2021). (3) Our data showed the differential expression patterns of hypoxia signaling pathway gene expressions between control and Pi groups. To further confirm our results, we could examine more hypoxia-related and Hif1 α target genes including ENO1, BHLHB2, and BNIP3 (Benita et al., 2009).

REFERENCES

- Aoyama, S., & Shibata, S. (2017). The Role of Circadian Rhythms in Muscular and Osseous Physiology and Their Regulation by Nutrition and Exercise. *Frontiers in Neuroscience, 11*, 63. doi:10.3389/fnins.2017.00063
- Aro, E., Salo, A. M., Khatri, R., Finnila, M., Miinalainen, I., Sormunen, R., . . . Myllyharju, J. (2015). Severe Extracellular Matrix Abnormalities and Chondrodysplasia in Mice Lacking Collagen Prolyl 4-Hydroxylase Isoenzyme II in Combination with a Reduced Amount of Isoenzyme I. *Journal of Biological Chemistry, 290*(27), 16964-16978. doi:10.1074/jbc.M115.662635
- Bais, M., McLean, J., Sebastiani, P., Young, M., Wigner, N., Smith, T., . . . Gerstenfeld, L. C. (2009). Transcriptional analysis of fracture healing and the induction of embryonic stem cell-related genes. *PLoS One, 4*(5), e5393. doi:10.1371/journal.pone.0005393
- Baldwin, C. T., Reginato, A. M., & Prockop, D. J. (1989). A new epidermal growth factor-like domain in the human core protein for the large cartilage-specific proteoglycan. Evidence for alternative splicing of the domain. *Journal of Biological Chemistry, 264*(27), 15747-15750.
- Benita, Y., Kikuchi, H., Smith, A. D., Zhang, M. Q., Chung, D. C., & Xavier, R. J. (2009). An integrative genomics approach identifies Hypoxia Inducible Factor-1 (HIF-1)-target genes that form the core response to hypoxia. *Nucleic Acids Research, 37*(14), 4587-4602. doi:10.1093/nar/gkp425

- Bentovim, L., Amarilio, R., & Zelzer, E. (2012). HIF1alpha is a central regulator of collagen hydroxylation and secretion under hypoxia during bone development. *Development*, *139*(23), 4473-4483. doi:10.1242/dev.083881
- Bilezikian, J. P. (2019). *Primer on the metabolic bone diseases and disorders of mineral metabolism*. In (pp. 1 online resource (1,136 pages)).
- Bonnarens, F., & Einhorn, T. A. (1984). Production of a standard closed fracture in laboratory animal bone. *Journal of Orthopaedic Research*, *2*(1), 97-101. doi:10.1002/jor.1100020115
- Boyle, W. J., Simonet, W. S., & Lacey, D. L. (2003). Osteoclast differentiation and activation. *Nature*, *423*(6937), 337-342. doi:10.1038/nature01658
- Bradham, D. M., Igarashi, A., Potter, R. L., & Grotendorst, G. R. (1991). Connective tissue growth factor: a cysteine-rich mitogen secreted by human vascular endothelial cells is related to the SRC-induced immediate early gene product CEF-10. *Journal of Cell Biology*, *114*(6), 1285-1294. doi:10.1083/jcb.114.6.1285
- Cui, C. B., Cooper, L. F., Yang, X., Karsenty, G., & Aukhil, I. (2003). Transcriptional coactivation of bone-specific transcription factor Cbfa1 by TAZ. *Molecular and Cellular Biology*, *23*(3), 1004-1013. doi:10.1128/MCB.23.3.1004-1013.2003
- Dallas, S. L., Prideaux, M., & Bonewald, L. F. (2013). The osteocyte: an endocrine cell ... and more. *Endocrine Reviews*, *34*(5), 658-690. doi:10.1210/er.2012-1026
- Ducy, P., & Karsenty, G. (1995). Two distinct osteoblast-specific cis-acting elements control expression of a mouse osteocalcin gene. *Molecular and Cellular Biology*, *15*(4), 1858-1869. doi:10.1128/MCB.15.4.1858

Ducy, P., Zhang, R., Geoffroy, V., Ridall, A. L., & Karsenty, G. (1997). *Osf2/Cbfa1*: a transcriptional activator of osteoblast differentiation. *Cell*, *89*(5), 747-754.

doi:10.1016/s0092-8674(00)80257-3

Einhorn, T. A. (1995). Enhancement of fracture-healing. *Journal of Bone and Joint Surgery*, *77*(6), 940-956. doi:10.2106/00004623-199506000-00016

Einhorn, T. A., & Gerstenfeld, L. C. (2015). Fracture healing: mechanisms and interventions. *Nature Review Rheumatology*, *11*(1), 45-54.

doi:10.1038/nrrheum.2014.164

Felsenfeld, A. J., & Levine, B. S. (2012). Approach to treatment of hypophosphatemia. *American Journal of Kidney Diseases*, *60*(4), 655-661. doi:10.1053/j.ajkd.2012.03.024

Fisher, L. W., McBride, O. W., Termine, J. D., & Young, M. F. (1990). Human bone sialoprotein. Deduced protein sequence and chromosomal localization. *Journal of Biological Chemistry*, *265*(4), 2347-2351.

Gerstenfeld, L. C., Cullinane, D. M., Barnes, G. L., Graves, D. T., & Einhorn, T. A. (2003). Fracture healing as a post-natal developmental process: molecular, spatial, and temporal aspects of its regulation. *Journal of Cellular Biochemistry*, *88*(5), 873-884.

doi:10.1002/jcb.10435

Holtrop, M. E., & King, G. J. (1977). The ultrastructure of the osteoclast and its functional implications. *Clinical Orthopaedics and Related Research* (123), 177-196.

Hussein, A. I., Carroll, D., Bui, M., Wolff, A., Matheny, H., Hogue, B., . . . Gerstenfeld, L. (2023). Oxidative metabolism is impaired by phosphate deficiency during fracture

healing and is mechanistically related to BMP induced chondrocyte differentiation. *Bone Reports*, 18, 101657. doi:10.1016/j.bonr.2023.101657

Kanai, F., Marignani, P. A., Sarbassova, D., Yagi, R., Hall, R. A., Donowitz, M., . . .

Yaffe, M. B. (2000). TAZ: a novel transcriptional co-activator regulated by interactions with 14-3-3 and PDZ domain proteins. *EMBO Journal*, 19(24), 6778-6791.

doi:10.1093/emboj/19.24.6778

Kessler, E., Takahara, K., Biniaminov, L., Brusel, M., & Greenspan, D. S. (1996). Bone morphogenetic protein-1: the type I procollagen C-proteinase. *Science*, 271(5247), 360-362. doi:10.1126/science.271.5247.360

Kobayashi, T., Soegiarto, D. W., Yang, Y., Lanske, B., Schipani, E., McMahon, A. P., & Kronenberg, H. M. (2005). Indian hedgehog stimulates periarticular chondrocyte differentiation to regulate growth plate length independently of PTHrP. *Journal of Clinical Investigation*, 115(7), 1734-1742. doi:10.1172/JCI24397

Komori, T., Yagi, H., Nomura, S., Yamaguchi, A., Sasaki, K., Deguchi, K., . . .

Kishimoto, T. (1997). Targeted disruption of *Cbfa1* results in a complete lack of bone formation owing to maturational arrest of osteoblasts. *Cell*, 89(5), 755-764.

doi:10.1016/s0092-8674(00)80258-5

Koo, J. H., & Guan, K. L. (2018). Interplay between YAP/TAZ and Metabolism. *Cell Metabolism*, 28(2), 196-206. doi:10.1016/j.cmet.2018.07.010

Koski, M. K., Anantharajan, J., Kursula, P., Dhavala, P., Murthy, A. V., Bergmann, U., . . . Wierenga, R. K. (2017). Assembly of the elongated collagen prolyl 4-hydroxylase

- alpha(2)beta(2) heterotetramer around a central alpha(2) dimer. *Biochemical Journal*, 474(5), 751-769. doi:10.1042/BCJ20161000
- Kronenberg, H. M. (2003). Developmental regulation of the growth plate. *Nature*, 423(6937), 332-336. doi:10.1038/nature01657
- Kunimoto, T., Okubo, N., Minami, Y., Fujiwara, H., Hosokawa, T., Asada, M., . . . Yagita, K. (2016). A PTH-responsive circadian clock operates in ex vivo mouse femur fracture healing site. *Scientific Reports*, 6, 22409. doi:10.1038/srep22409
- Li, S. W., Sieron, A. L., Fertala, A., Hojima, Y., Arnold, W. V., & Prockop, D. J. (1996). The C-proteinase that processes procollagens to fibrillar collagens is identical to the protein previously identified as bone morphogenic protein-1. *Proceedings of the National Academy of Sciences of the United States of America*, 93(10), 5127-5130. doi:10.1073/pnas.93.10.5127
- Li, Y., Yang, S., Qin, L., & Yang, S. (2021). TAZ is required for chondrogenesis and skeletal development. *Cell Discovery*, 7(1), 26. doi:10.1038/s41421-021-00254-5
- Liamis, G., Milionis, H. J., & Elisaf, M. (2010). Medication-induced hypophosphatemia: a review. *QJM*, 103(7), 449-459. doi:10.1093/qjmed/hcq039
- Mansfield, K., Rajpurohit, R., & Shapiro, I. M. (1999). Extracellular phosphate ions cause apoptosis of terminally differentiated epiphyseal chondrocytes. *Journal of Cellular Physiology*, 179(3), 276-286. doi:10.1002/(SICI)1097-4652(199906)179:3<276::AID-JCP5>3.0.CO;2-#
- Marsell, R., & Einhorn, T. A. (2011). The biology of fracture healing. *Injury*, 42(6), 551-555. doi:10.1016/j.injury.2011.03.031

- Maruyama, M., Rhee, C., Utsunomiya, T., Zhang, N., Ueno, M., Yao, Z., & Goodman, S. B. (2020). Modulation of the Inflammatory Response and Bone Healing. *Frontiers in Endocrinology (Lausanne)*, *11*, 386. doi:10.3389/fendo.2020.00386
- Michigami, T., & Ozono, K. (2019). Roles of Phosphate in Skeleton. *Frontiers in Endocrinology (Lausanne)*, *10*, 180. doi:10.3389/fendo.2019.00180
- Nagaraj, R., Gururaja-Rao, S., Jones, K. T., Slattery, M., Negre, N., Braas, D., . . . Banerjee, U. (2012). Control of mitochondrial structure and function by the Yorkie/YAP oncogenic pathway. *Genes and Development*, *26*(18), 2027-2037. doi:10.1101/gad.183061.111
- Noguchi, T., Hussein, A. I., Horowitz, N., Carroll, D., Gower, A. C., Demissie, S., & Gerstenfeld, L. C. (2018). Hypophosphatemia Regulates Molecular Mechanisms of Circadian Rhythm. *Scientific Reports*, *8*(1), 13756. doi:10.1038/s41598-018-31830-7
- Okubo, N., Minami, Y., Fujiwara, H., Umemura, Y., Tsuchiya, Y., Shirai, T., . . . Yagita, K. (2013). Prolonged bioluminescence monitoring in mouse ex vivo bone culture revealed persistent circadian rhythms in articular cartilages and growth plates. *PLoS One*, *8*(11), e78306. doi:10.1371/journal.pone.0078306
- Ortega, N., Behonick, D. J., & Werb, Z. (2004). Matrix remodeling during endochondral ossification. *Trends in Cell Biology*, *14*(2), 86-93. doi:10.1016/j.tcb.2003.12.003
- Orwoll, E. S. (2003). Toward an expanded understanding of the role of the periosteum in skeletal health. *Journal of Bone and Mineral Research*, *18*(6), 949-954. doi:10.1359/jbmr.2003.18.6.949

- Percival, C. J., & Richtsmeier, J. T. (2013). Angiogenesis and intramembranous osteogenesis. *Developmental Dynamics*, 242(8), 909-922. doi:10.1002/dvdy.23992
- Provot, S., Zinyk, D., Gunes, Y., Kathri, R., Le, Q., Kronenberg, H. M., . . . Schipani, E. (2007). Hif-1alpha regulates differentiation of limb bud mesenchyme and joint development. *Journal of Cellular Biology*, 177(3), 451-464. doi:10.1083/jcb.200612023
- Pucci, B., Adams, C. S., Fertala, J., Snyder, B. C., Mansfield, K. D., Tafani, M., . . . Shapiro, I. M. (2007). Development of the terminally differentiated state sensitizes epiphyseal chondrocytes to apoptosis through caspase-3 activation. *Journal of Cellular Physiology*, 210(3), 609-615. doi:10.1002/jcp.20857
- Sabbagh, Y., Carpenter, T. O., & Demay, M. B. (2005). Hypophosphatemia leads to rickets by impairing caspase-mediated apoptosis of hypertrophic chondrocytes. *Proceedings of the National Academy of Sciences of the United States of America*, 102(27), 9637-9642. doi:10.1073/pnas.0502249102
- Safadi, F. F., Xu, J., Smock, S. L., Kanaan, R. A., Selim, A. H., Odgren, P. R., . . . Popoff, S. N. (2003). Expression of connective tissue growth factor in bone: its role in osteoblast proliferation and differentiation in vitro and bone formation in vivo. *Journal of Cellular Physiology*, 196(1), 51-62. doi:10.1002/jcp.10319
- Scott, I. C., Blitz, I. L., Pappano, W. N., Imamura, Y., Clark, T. G., Steiglit, B. M., . . . Greenspan, D. S. (1999). Mammalian BMP-1/Tolloid-related metalloproteinases, including novel family member mammalian Tolloid-like 2, have differential enzymatic activities and distributions of expression relevant to patterning and skeletogenesis. *Developmental Biology*, 213(2), 283-300. doi:10.1006/dbio.1999.9383

Shi, N., Foley, K., Lenhart, G., & Badamgarav, E. (2009). Direct healthcare costs of hip, vertebral, and non-hip, non-vertebral fractures. *Bone*, *45*(6), 1084-1090.

doi:10.1016/j.bone.2009.07.086

Sivaraj, K. K., Dharmalingam, B., Mohanakrishnan, V., Jeong, H. W., Kato, K., Schroder, S., . . . Adams, R. H. (2020). YAP1 and TAZ negatively control bone angiogenesis by limiting hypoxia-inducible factor signaling in endothelial cells. *Elife*, *9*.

doi:10.7554/eLife.50770

Sommerfeldt, D. W., & Rubin, C. T. (2001). Biology of bone and how it orchestrates the form and function of the skeleton. *European Spine Journal*, *10 Suppl 2*(Suppl 2), S86-95.

doi:10.1007/s005860100283

Sozen, T., Ozisik, L., & Basaran, N. C. (2017). An overview and management of osteoporosis. *European Journal of Rheumatology*, *4*(1), 46-56.

doi:10.5152/eurjrheum.2016.048

Sudol, M., Bork, P., Einbond, A., Kastury, K., Druck, T., Negrini, M., . . . Lehman, D. (1995). Characterization of the mammalian YAP (Yes-associated protein) gene and its role in defining a novel protein module, the WW domain. *Journal of Biological Chemistry*, *270*(24), 14733-14741. doi:10.1074/jbc.270.24.14733

doi:10.1074/jbc.270.24.14733

Uhlen, M., Fagerberg, L., Hallstrom, B. M., Lindskog, C., Oksvold, P., Mardinoglu, A., . . . Ponten, F. (2015). Proteomics. Tissue-based map of the human proteome. *Science*,

347(6220), 1260419. doi:10.1126/science.1260419

Vaananen, H. K., Zhao, H., Mulari, M., & Halleen, J. M. (2000). The cell biology of osteoclast function. *Journal of Cell Science*, *113 (Pt 3)*, 377-381.

doi:10.1242/jcs.113.3.377

Vanyai, H. K., Prin, F., Guillermin, O., Marzook, B., Boeing, S., Howson, A., . . .

Thompson, B. (2020). Control of skeletal morphogenesis by the Hippo-YAP/TAZ pathway. *Development*, *147(21)*. doi:10.1242/dev.187187

von Eyss, B., Jaenicke, L. A., Kortlever, R. M., Royle, N., Wiese, K. E., Letschert, S., . . .

Eilers, M. (2015). A MYC-Driven Change in Mitochondrial Dynamics Limits YAP/TAZ Function in Mammary Epithelial Cells and Breast Cancer. *Cancer Cell*, *28(6)*, 743-757.

doi:10.1016/j.ccell.2015.10.013

Wigner, N. A., Luderer, H. F., Cox, M. K., Sooy, K., Gerstenfeld, L. C., & Demay, M. B.

(2010). Acute phosphate restriction leads to impaired fracture healing and resistance to BMP-2. *Journal of Bone and Mineral Research*, *25(4)*, 724-733.

doi:10.1359/jbmr.091021

Zarka, M., Hay, E., & Cohen-Solal, M. (2021). YAP/TAZ in Bone and Cartilage Biology. *Frontiers in Cell and Developmental Biology*, *9*, 788773.

doi:10.3389/fcell.2021.788773

Zvonic, S., Ptitsyn, A. A., Kilroy, G., Wu, X., Conrad, S. A., Scott, L. K., . . . Gimble, J.

M. (2007). Circadian oscillation of gene expression in murine calvarial bone. *Journal of Bone and Mineral Research*, *22(3)*, 357-365. doi:10.1359/jbmr.061114

VITA

